ARTICLES

Femtosecond Fluorescence Studies of Self-Assembled Helical Aggregates in Solution

Paul Toele,‡ Judith J. van Gorp,§ and Max Glasbeek*,‡

Laboratory for Physical Chemistry, University of Amsterdam, Nieuwe Achtergracht 129, 1018 WS Amsterdam, The Netherlands, and Laboratory of Macromolecular and Organic Chemistry, Eindhoven University of Technology, P.O. Box 513, 5600 MB Eindhoven, The Netherlands

Received: June 21, 2005; In Final Form: September 22, 2005

For the diamino-bipyridine based C_3-symmetrical disk molecule, TAB, (sub)picosecond fluorescence transients have been observed by means of femtosecond fluorescence upconversion and picosecond time-correlated photon counting techniques. The dodecyl peripheral side chains of the synthetic compound are large enough to allow, in apolar solvents, self-assembling of the discotic molecules to helical aggregates. In polar solvents, the hydrogen bonding and $\pi-\pi$ interactions pertaining to the chiral aggregation are compensated by solvation and self-assembling of the disklike molecules is disrupted. For comparison, time-resolved fluorescence measurements have been performed for the subgroup molecule, DAC, which is the (asymmetric) building block for TAB. It is concluded that, after pulsed photoexcitation, TAB and DAC exhibit excited-state intramolecular double proton transfer (ESIDPT) with a typical time of ∼200−300 fs, irrespective of the degree of aggregation. Picosecond components in the fluorescence of TAB and DAC, ranging from 3 to 25 ps, are representative of vibrational cooling effects in the excited product state. Only aggregated TAB shows a rapid (∼1 ps) decay of its fluorescence anisotropy. This component is attributed to excited-state energy transfer within the aggregate. Finally, the excited-state lifetime of TAB in the aggregated form is found to be an order of magnitude longer than that for TAB in its nonaggregated form. It is inferred that aggregation diminishes the influence of low-frequency twisting motions in the radiationless decay of the excited state.

Introduction

Recently chirality of self-assembled stacks of C_3-symmetrical disk-shaped molecules in polar protic solvents was reported.[1] The synthetic compounds possess large peripheral side chains that serve as a shield for the inner part of the stacks against direct contact with the solvent molecules. Stacking of the molecular disks results from secondary interactions among neighboring molecules. Chirality of the supramolecules is due to the typical propeller-like structure of the assembled molecular disks.[2]

For the C_3-symmetrical disk-shaped molecule **1a** (Chart 1) it has been shown that cooperative intermolecular $\pi-\pi$ interactions and intermolecular hydrogen bonding are crucial for columnar aggregation in apolar alkane solution.[2] In **1a**, the three functional diamino-bipyridyl groups are wedged onto the central group and mutually twisted. Stacking of the disks inherently renders disk rotation and expression of helicity.[2] On the other hand, in polar media, solvation compensates for the secondary interactions and self-assembling of the disklike molecules is disrupted.[2]

In recent years, numerous optical spectroscopic studies of polymers, aggregates, and dendrimers have been undertaken.[3−20] In these studies the role of interchromophore interactions, e.g., Coulombic exchange and dipole−dipole couplings, in determining the optical spectra has been emphasized. Interchromophore interactions are also of vital importance for the dynamic processes ensuing photoexcitation of the multichromophore species. Coherent collective electronic (viz. excitonic) excitation or incoherent energy hopping among neighboring chromophores in the aggregate are issues of central interest.[7,21−24] Typically, the time scales of these processes span several orders of magnitude, from tens of femtoseconds to hundreds of picoseconds, thus requiring ultrafast spectroscopic methods for the probing of the excited-state dynamics in real time.[9,22,25−27] In particular, if the stacks are fluorescent, the femtosecond fluorescence upconversion technique should be promising because with this technique the temporal behavior of only the excited-state population is studied, without the interference of bleaching and excited-state absorption phenomena as in ultrafast transient absorption experiments.[27−29]

In this paper we present results of a femtosecond fluorescence upconversion study of the C_3-symmetrical disk molecule TAB (**1a**) and the subgroup molecule DAC (**2a**). In both molecular systems, the fluorescence is from the photoexcited diamino-bipyridyl functional groups. In apolar solvents, only **1a** exhibits columnar self-assembled stacking; molecule **2a** does not show aggregation.[2] Time-resolved fluorescence data for **1a** in aggregated and nonaggregated forms therefore should enable us to compare the dynamics of the fluorescent diamino-bipyridyl functional groups in the different stages of aggregation. Furthermore, the dynamics of the supramolecular entities **1a** can be compared with that of the subgroup **2a**. It will be shown

* Address correspondence to this author. E-mail: glasbeek@science.uva.nl.
‡ University of Amsterdam.
§ Eindhoven University of Technology.

10.1021/jp053339m CCC: $30.25
Published on Web 10/27/2005

CHART 1: Molecular Structures of TAB (1a) and the Subgroup Molecule DAC (2a)

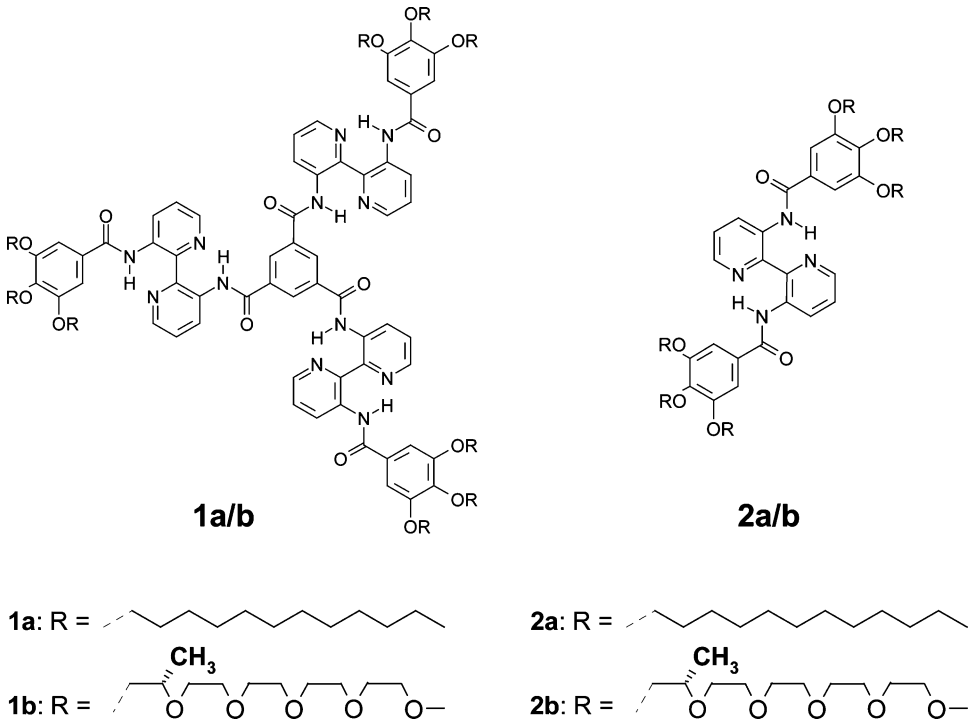

that for all solutions investigated the fluorescence transients exhibit multiexponential decays with time constants ranging from a few tens of femtoseconds to nanoseconds. The main structural difference between compounds **1a** and **2a**, on one hand, and the analogous compounds **1b** and **2b** studied previously,[1] on the other hand, is that in **1a** and **2a** the peripheral groups attached to the diamino-bipyridyl entities are apolar and that in **1b** and **2b** the end groups are polar (hence the difference in aggregation behavior with respect to solvent polarity). The presence of diamino-bipyridyl groups is common to all molecules **1a**−**2b**. Previously, it has been discussed for **1b** and **2b** that pulsed photoexcitation induced intramolecular double proton transfer within the diamino-bipyridyl groups, regardless of the degree of aggregation of the disk-type molecule.[1] Likewise, the data of the subpicosecond experiments presented here reveal rapid excited-state tautomerization for **1a** and **2a**; the characteristic transfer time (for the proton translocation from the amide to the nitrogen in the heterocycle) is found as ∼300 fs. In addition, on a picosecond time scale, the fluorescence transients of DAC and TAB, irrespective of the degree of aggregation of the latter, are found to contain components with typical times ranging from 3 to 25 ps. It will be discussed that these components originate from vibrational cooling of the solute molecules in the solvent bath.

Moreover, we have studied the time dependence of the polarization of the fluorescence of the emissive molecules, in the aggregated and nonaggregated forms. As is well-known, such experiments may provide useful information concerning the dynamics of the reorientational motions of the probed molecules in the solution or, in the event that the depolarization is faster than rotational diffusion, information regarding rapid directional changes of the optical transition dipole moment due to rapid intramolecular relaxation.[9,13,30] We find that only aggregated TAB shows a rapid (∼1 ps) decay of its fluorescence anisotropy; this component is not observed for nonaggregated TAB and DAC. It is argued that the ∼1 ps fluorescence anisotropy decay component is evidence for excited-state energy transfer within the aggregated assemblies. Vibrational cooling of "hot" molecules in the solution is discussed to also contribute to fluorescence depolarization (∼20 ps), while for all species a long-lived residual fluorescence anisotropy is found showing that depolarization due to reorientational motions of the molecules (stacks) in the solution is slow compared to the excited-state lifetime.

Experimental Section

DAC and TAB compounds were synthesized as described elsewhere.[31] The solvents, *n*-heptane (Acros Organics) and chloroform (Merck), were of spectrograde quality. Measurements were performed with $\sim 10^{-3}-10^{-4}$ M solutions. Steady-state absorption spectra were recorded with a Shimadzu UV-240 spectrophotometer. Steady-state fluorescence spectra were obtained by using the emission spectrometer described elsewhere.[32] Fluorescence transients, with time windows up to 60 ps, were recorded by means of the femtosecond fluorescence upconversion apparatus described previously.[30] In these experiments, a passively mode-locked Tsunami Ti:sapphire laser was optically pumped by a cw Nd:YVO4 diode laser (Spectra Physics, Millennia X), producing 60 fs pulses (fwhm) at 800 nm wavelength, at a repetition rate of 82 MHz. Amplification of the output pulse energy was accomplished by using a regenerative amplifier (RGA) laser system (Quantronix), which generated 100 fs pulses (fwhm) at a repetition rate of 1 kHz and a mean pulse energy of 500 μJ. Two laser beams were produced by passage of the output pulses through a beam splitter. One beam was used to pump an optical parametric amplifier (OPA) laser system (TOPAS; Light Conversion Ltd.). The third harmonic of the wavelength tunable output pulses of the TOPAS laser system was used as the excitation source; the wavelength could be varied between 310 and 380 nm and the mean output pulse energy was ∼5 μJ. To circumvent local heating of the sample by the excitation pulses, the 1 mm quartz cell containing the sample was put in a sample holder that was driven back-and-forth by an electromotor. The second beam, the gating beam, was led through the optical delay line

containing a stepper-motor driven translational stage. The transient fluorescence originating from the sample was focused onto a BBO crystal together with the gating beam (800 nm), to generate the sum-frequency signal (type I phase matching condition). The sum-frequency signal was led through a UG 11 band-pass filter and focused onto the entrance slit of a Zeiss M4 prism monochromator. The spectrally dispersed signal was detected with use of a photomultiplier tube (EMI 9863 QB/350). The photomultiplier output was connected to a lock-in amplifier that was synchronized with an electronic reference signal of the RGA laser system. The output signal of the lock-in detector was stored and analyzed by means of a personal computer. Time-resolved emission spectra were obtained by applying the spectral reconstruction method.[30,33] In this method, time zero is well defined and, unlike in the direct measurement of time-resolved emission spectra, additional corrections for group velocity dispersion are not necessary.[27,28] The system response time was determined to be 300 ± 20 fs by measuring the cross-correlation signal of the gate and excitation beams, at 800 and 380 nm, respectively.

A linear polarizer in the excitation pathway was used to vary the polarization direction of the excitation pulses relative to the vertically polarized gating-beam pulses. To exclude fluorescence decay effects due to rotational diffusion motions of the solute molecules in the liquid, the fluorescence intensity was measured under magic angle conditions (with the laser-excitation polarization at an angle of 54.7° relative to the vertically polarized gating beam).[34] Additionally, time-resolved depolarization measurements were performed with the polarizer at parallel and perpendicular polarization configurations to measure the fluorescence anisotropy, $r(t)$, which has the usual meaning, $r(t) = (I_{||} - I_{\perp})/(I_{||} + 2I_{\perp})$.

A second laser system, outfitted with a time-correlated single-photon-counting (TCSPC) detection system, was used for the measurement of fluorescence transients in a time span of 15 ps to 10 ns. Details of the setup are given elsewhere.[32] Extension of the time window to the picosecond-to-nanosecond range is essential for the calibration of the intensities of the transients obtained in the femtosecond measurements. A mode-locked Ar^+-ion laser (Coherent, Innova 200-15) synchronously pumped a dye laser (Coherent, 702−3) outfitted with a cavity dumper (Coherent, 7200). The cavity-dumped dye laser generated laser pulses with a duration of ∼1 ps (fwhm autocorrelation trace), an energy of about 25 nJ/pulse, and a repetition rate of 3.7 MHz. These pulses were frequency doubled in a 6 mm BBO crystal, yielding pulses at a wavelength of 323 nm to photoexcite the sample. The fluorescence emitted from the sample in a direction perpendicular to the excitation beam was focused onto the entrance slit of a monochromator outfitted with a multichannel plate photodetector. A linear polarizer was inserted in the detection pathway to detect the intensity of the parallel and perpendicular polarized transients and at magic angle conditions. The instrumental response time of the TCSPC setup was about 17 ps (fwhm).

Results

DAC. Figure 1 shows the steady-state absorption and emission spectrum for DAC in *n*-heptane. For DAC in (polar) chloroform the same spectra were obtained. The peak intensities for the main absorption bands occur near ∼350 and ∼290 nm; the bands are due to S_0-S_1 and S_0-S_2 transitions, respectively. Semiempirical AM1 and ab initio configuration interaction (CI) calculations were performed with the Spartan 5.0 software package. The calculations revealed that the S_0-S_1 transition

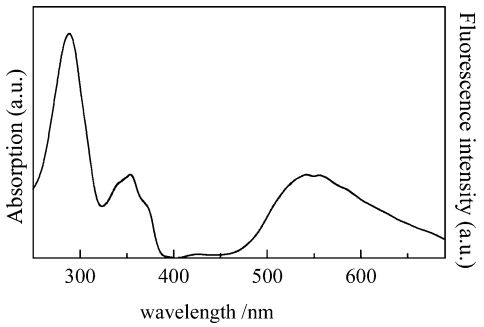

Figure 1. Steady-state absorption and emission (excitation at 323 nm) spectra of DAC (**2a**) in *n*-heptane.

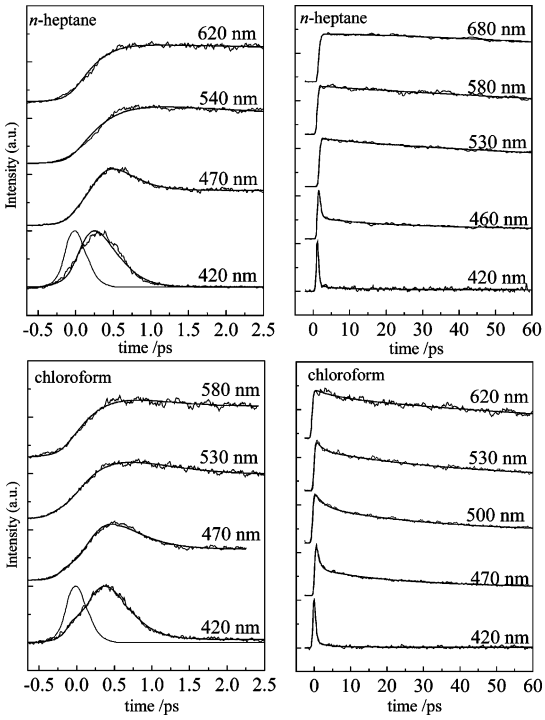

Figure 2. Femtosecond fluorescence upconversion transients of DAC in *n*-heptane and chloroform. Detection wavelengths are indicated. The excitation wavelength was at 350 nm.

predominantly involves a $\pi \rightarrow \pi^*$ HOMO−LUMO excitation on the diamino-bipyridyl group. The fluorescence spectrum (excitation at ∼323 nm) consists of a strong band, with a maximum at ∼550 nm, and a weak band (weaker by an order of magnitude), peaking near 420 nm. As discussed later, the weak band is attributed to emission from the S_1 state, whereas the strong band emission (positioned ∼10 000 cm^{-1} to the red of the S_0-S_1 absorption) is attributed to the DAC molecule after excited-state intramolecular double proton transfer (vide infra).

Femtosecond fluorescence upconversion transients were measured for DAC, dissolved in *n*-heptane and chloroform, using time windows of 3 and 60 ps. Typical results are shown in Figure 2. The figure also shows the instrumental response function at short time windows. Following the fitting and global analysis procedure described previously,[30,33] each transient was fitted to a multiexponential function convoluted with the instrumental response function. To scale the decay transients of the upconversion experiments to the decay transients obtained in the TCSPC experiments, the long lifetime decay component (τ_4), as determined by means of the TCSPC setup, was included in the multiexponential fit, $I(\lambda,t)$, for the upconversion transients. The best-fit transients are included as solid lines in Figure 2;

TABLE 1: Characteristic Times of Multiexponential Best-Fits to Femtosecond Fluorescence Upconversion Transients Observed for DAC (2a) in *n*-Heptane and Chloroform[a]

fluorescence wavelength/nm	τ_1/ps	τ_2/ps	τ_3/ps	τ_4/ps
		n-heptane		
420		0.19 (0.97)	5.1 (0.02)	200[b] (0.01)
460	0.15 (−1)	0.34 (0.46)	21 (0.06)	200[b] (0.48)
530	0.13 (−1)		17 (0.06)	200[b] (0.94)
580	0.20 (−1)			200[b] (1)
680	0.20 (−0.9)		24 (−0.1)	200[b] (1)
		chloroform		
420	0.15 (−1)	0.25 (0.94)	3.0 (0.05)	120[b] (0.01)
470	0.18 (−1)	0.72 (0.62)	15 (0.18)	120[b] (0.20)
500	0.15 (−1)	2.5 (0.34)	21 (0.22)	120[b] (0.44)
530	0.20 (−1)	1.6 (0.23)	24 (0.25)	120[b] (0.52)
620	0.20 (−1)	2.4 (0.08)		120[b] (0.92)

[a] Relative intensities are given in parentheses. [b] Values normalized to picosecond time-correlated single-photon detection experiments.

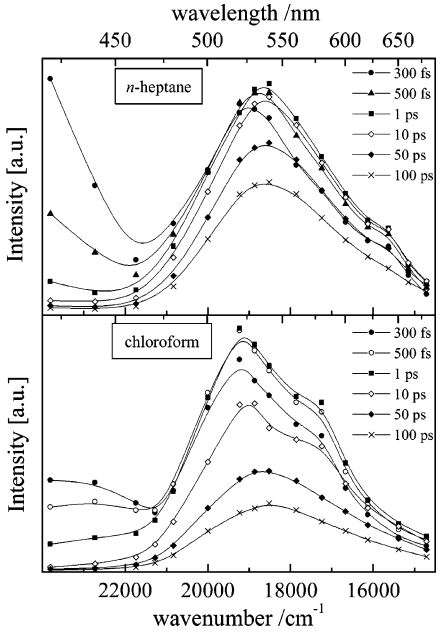

Figure 3. Reconstructed time-resolved fluorescence spectra of DAC dissolved in *n*-heptane (upper panel) and chloroform (lower panel) for the indicated delay times.

the corresponding best-fit parameter values are given in Table 1. To construct the time-resolved spectra, the integrated intensity of the fluorescence transients, $\int_0^\infty I(\lambda,t)\,dt$, was scaled to the intensity $I_c(\lambda)$ of the calibrated steady-state emission spectrum. The latter was obtained by using the TCSPC setup that had been calibrated to correct for the variation of the detection sensitivity with the detection wavelength.[32] Finally, the spectrum at time t could be reconstructed as a point-to-point plot from the scaled functions, $I_s(\lambda,t)$, obtained for a series of different detection wavelengths λ.

The time dependence of the emission spectrum (Figure 3) shows several features. At the earliest times (up to about 1 ps), the emission spectrum shows a rapidly decaying band emission in the region 420−460 nm. Upconversion transients at a detection wavelength below 420 nm could not be measured with our setup. From the shape of the emission band near 420 nm, it is inferred that the maximum of the short-living emission is below 420 nm. For DAC dissolved in *n*-heptane, the band emission near 420 nm decays with a time of ∼200 fs. Concomitantly, the band near 530 nm shows a rise and a red shift by ∼500 cm^{-1}. After ∼1 ps, the 530 nm band emission shows an overall decay with a typical time of approximately 200 ps and also the band structure disappears and is slightly narrowed in a time of ∼20 ps.

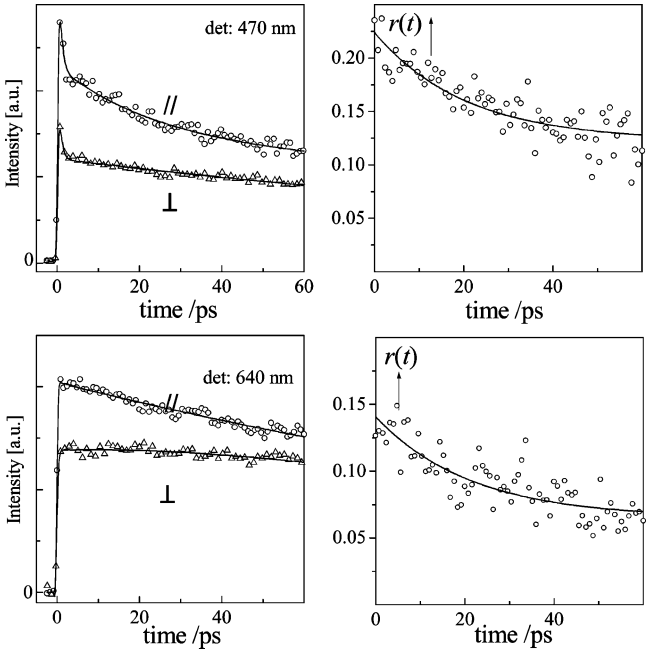

Figure 4. Polarized fluorescence upconversion transients of DAC, dissolved in *n*-heptane, for excitation at 380 nm and detection at 470 and 640 nm (left) and the corresponding fluorescence depolarization curves (right). Solid lines are best-fits to multiexponential functions.

For the time dependence of the emission spectrum of DAC in chloroform a somewhat different behavior was observed. The fast decaying band near 420 nm now shows a nonuniform decay, with a time of ∼200 fs at the low-wavelength side and a time of ∼700 fs when detection is near 450 nm. Concomitant with the decay of the 420 nm emission, the emission near 530 nm shows a rise. The results reflect a dynamic Stokes shift, this shift being ∼700 cm^{-1}. After about 10 ps, the 530 nm emission decays with a time constant of ∼120 ps. Initially, the 530 nm band emission shows some vibrational structure that is lost after ∼50 ps; beyond this time the shape of the emission band equals that for steady-state emission.

The temporal behavior of the parallel and perpendicular polarized components of the fluorescence upconversion transients of DAC was also measured. To avoid monitoring fluorescence depolarization other than that due to proton transfer (vide infra), the wavelength of the exciting laser pulses was chosen near the origin of the S_0-S_1 absorption, at 380 nm. Detection of the polarized transients was reliable at wavelengths of 470 nm (lower limit) and higher. (The cutoff filter in the detection pathway prevents the detection of fluorescence at wavelengths shorter than 460 nm.) Figure 4 shows fluorescence upconversion transients of DAC in *n*-heptane, for parallel and perpendicular polarized emission with respect to the polarization of the 380 nm excitation pulses. Clearly, the polarized transients detected at 470 nm show a very rapid initial decay component (∼200 fs), which is more pronounced in the parallel-polarized than in the perpendicular-polarized transient. As detailed later, this fast component is reminiscent of a very fast decay of DAC in the reactant state due to excited-state intramolecular double proton transfer (ESIDPT). It should be added, however, that the initial anisotropy value measured at 470 nm does not simply give the fluorescence anisotropy of DAC in the reactant state prior to ESIDPT, since the fluorescence intensity at this

TABLE 2: Best-Fit Parameter Values for Temporal Dependence of the Fluorescence Anisotropy of DAC in *n*-Heptane and Chloroform[a]

solvent	detection/nm	anisotropy $r(0)$	time constant τ_1/ps	τ_2/ps
n-heptane	470	0.22	20 (0.55)	~300 ps (0.45)
	640	0.15	21 (0.46)	~300 ps (0.54)
chloroform	470	0.20	21 (0.58)	~400 ps (0.42)

[a] Relative weights are given in parentheses.

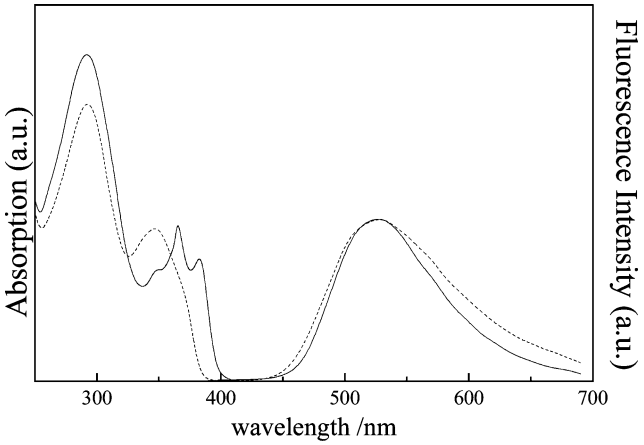

Figure 5. Steady-state absorption and emission spectra of TAB in *n*-heptane (solid line) and chloroform (dashed line).

wavelength is due to the overlap of the 420 and 530 nm band emissions, these bands being due to the reactant and product states, respectively. The measured fluorescence anisotropy showed biexponential decay behavior. For DAC dissolved in chloroform similar transients were measured. Best-fit parameter values are summarized in Table 2.

TAB. Steady-state absorption and emission spectra of TAB in *n*-heptane and chloroform were measured (Figure 5). In *n*-heptane, TAB exists in part in an aggregated form, and in chloroform, TAB is nonaggregated.[2] For TAB dissolved in *n*-heptane the absorption near 365 nm is structured, this structure being absent when chloroform is used as a solvent. The absorption in this spectral region is attributed to the S_0-S_1 transition. The absorption band at ~290 nm is attributed to the S_0-S_2 transition. The broad fluorescence band has a maximum near 530 nm.

Fluorescence upconversion transients were measured with time windows of 3, 10, and 60 ps. Representative transients

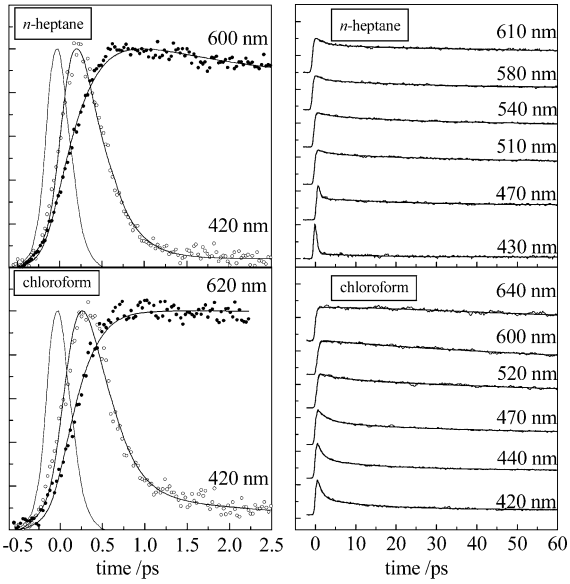

Figure 6. Fluorescence upconversion transients of TAB in *n*-heptane and chloroform, emission wavelength as indicated. Time windows: 3 ps (left panel) and 60 ps (right panel). Excitation was at 350 nm.

obtained at a series of detection wavelengths are given in Figure 6. Best-fits to convoluted multiexponential functions were obtained as before and are included in the figure as drawn lines. The corresponding time constants and relative weights are given in Table 3. $\tau_1-\tau_3$ were obtained with the upconversion technique, and τ_4 and τ_5 followed from the calibrated TCSPC results presented below. As illustrated in Figure 6, the early time kinetics of the fluorescence of TAB is different for the detection wavelengths at 420 and 620 nm. At 420 nm, an "instantaneous" rise (limited by the system response) is followed by a decay with a typical time of about 300 fs. At 620 nm, however, a rise with a time constant of ~300 fs for TAB in *n*-heptane (~200 fs when the solvent is chloroform) is clearly resolved. As for DAC, the variation of the rise and decay kinetics of the fluorescence with the detection wavelength is reflected in the temporal behavior of the spectra that were obtained after spectral reconstruction. Figure 7 shows the results for TAB dissolved in *n*-heptane and chloroform. When the solvent is *n*-heptane, a blue band emission (λ < 450 nm) is observed for times shorter than ~1 ps. This band emission has a characteristic decay time of ~300 fs. Concomitant with this decay, the ~530 nm band emission shows an increase. This

TABLE 3: Characteristic Times of Multiexponential Best-Fits to Femtosecond Fluorescence Upconversion Transients Observed for TAB (1a) in *n*-Heptane and Chloroform[a]

fluorescence wavelength/nm	τ_1/ps	τ_2/ps	τ_3/ps	τ_4/ps	τ_5/ps
			n-heptane		
430	0.05 (−0.80)	0.30 (0.85)	12 (0.03)		4000[b] (0.02)
470	0.15 (−1)	0.38 (0.52)	9.3 (0.10)		4000[b] (0.38)
510	0.30 (−1)	2.4 (0.12)		160 (0.10)	4000[b] (0.78)
540	0.29 (−1)	2.6 (0.10)	16 (0.10)	85 (0.10)	4000[b] (0.70)
580	0.29 (−1)	1.0 (0.20)	29 (0.15)		4000[b] (0.65)
610	0.30 (−1)	2.6 (0.29)		84 (0.20)	4000[b] (0.51)
			chloroform		
420	0.05 (−1)	0.33 (0.80)	6.4 (0.14)		400[b] (0.06)
440	0.15 (−1)	0.85 (0.55)	11 (0.20)	50 (0.08)	400[b] (0.17)
470	0.15 (−1)	2.2 (0.36)	13 (0.16)	140 (0.17)	400[b] (0.10)
520	0.16 (−1)	2.4 (0.20)		150 (0.26)	400[b] (0.54)
600	0.20 (−1)			96 (0.50)	400[b] (0.50)
640	0.20 (−0.90)		11 (−0.10)	100 (0.56)	400[b] (0.44)

[a] Relative intensities are given in parentheses. [b] Values normalized to picosecond time-correlated single-photon detection experiments.

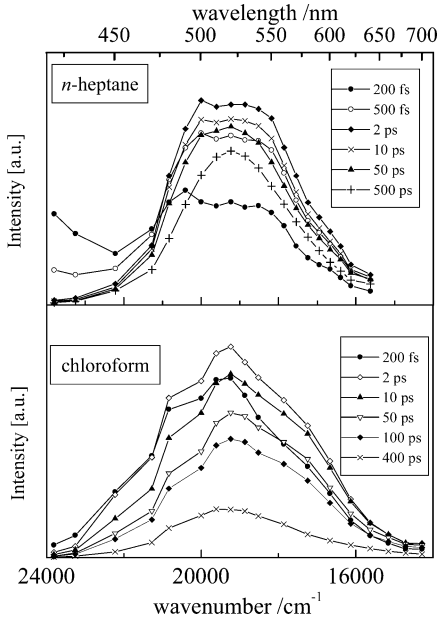

Figure 7. Reconstructed fluorescence spectra of TAB in *n*-heptane and chloroform; time delays after pulsed excitation (at 350 nm) are given in inserts.

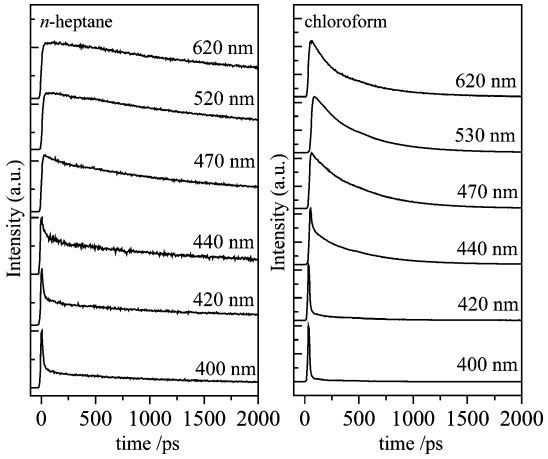

Figure 8. Fluorescence transients of TAB in *n*-heptane (left panel) and in chloroform (right panel) as probed with the TCSPC apparatus.

behavior is similar to that observed for the 530 nm band of DAC. Subsequently, the 530 nm band shows a decay and also changes of its band shape (see, e.g., the band shapes at delay times of 200 fs and 10 ps). At early times, the band is broad and may even be comprised of vibrational structure, whereas at later times (t > 10 ps) the band shape resembles that of the steady-state emission. Similar results were observed for TAB dissolved in chloroform although now the blue-band emission (λ < 420 nm) is not spectrally resolved.

Fluorescence lifetime measurements (on a (sub-) nanosecond time scale) were performed with the time-correlated single-photon counting fluorescence spectrometer. Figure 8 shows illustrative transients for TAB in the aggregated form (in *n*-heptane) and nonaggregated form (in chloroform). In contrast to the DAC results, a strong influence of the solvent polarity on the fluorescence lifetime of TAB was observed. In chloroform, the fluorescent-state lifetime (for nonaggregated TAB) was approximately 400 ps, i.e., the same order of magnitude as the lifetime of the fluorescent state of DAC. For TAB in *n*-heptane, however, the lifetime of the emissive state is found

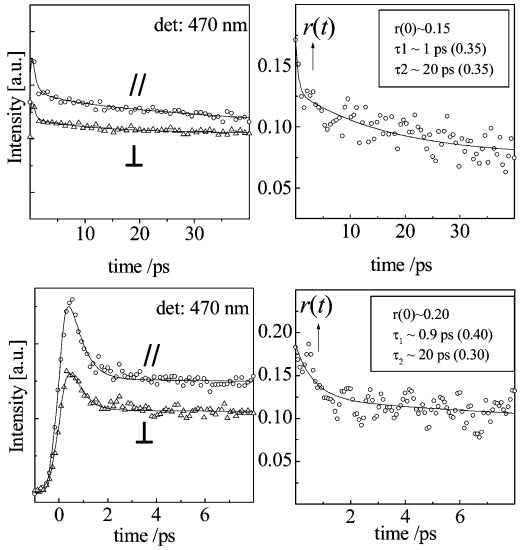

Figure 9. Polarized fluorescence upconversion transients of TAB, dissolved in *n*-heptane, for excitation at 380 nm and detection at 470 nm, with time windows of 8 and 40 ps (left). The time dependence of the corresponding fluorescence anisotropy is given in the panels on the right. Solid lines are best fits to multiexponential functions.

as 4 ns. Thus upon aggregation the lifetime of the excited S_1 state is lengthened by an order of magnitude.

Finally, we present in Figure 9 the parallel- and perpendicular-polarized fluorescence upconversion transients as detected for TAB, in *n*-heptane, at 470 nm, for time windows of 8 and 40 ps, respectively. From these transients we find an initial anisotropy of $r(0) = 0.25$, which decays biexponentially, with characteristic times of ~1 (35%) and ~20 ps (35%). The best-fit functions are given by the drawn lines in the figure. The lifetime of the residual anisotropy (~0.07) for aggregated TAB was longer than 4 ns.

Discussion

The spectral properties of DAC in liquid solution are similar to those of 2,2′-bipyridyl-3,3′-diol ($BP(OH)_2$) studied in detail.[30,35−38] As for $BP(OH)_2$, the positions of the absorption and emission bands (at ~350 and ~550 nm, respectively) are insensitive to the polarity of the solvent and also the two bands are separated by about 10 000 cm^{-1}. These features are indicative of (i) a small disparity in the dipole moments of the initial and final states involved in the absorptive and emissive transitions and (ii) the appreciable difference of the emissive state from that initially excited. For $BP(OH)_2$, the observations confirmed the idea of an excited-state intramolecular double proton transfer (ESIDPT) process[30,35−38] that was already inferred previously from electrooptical experiments[39,40] and quantum mechanical calculations.[41,42] Likewise, we assign the 530 nm emission band of DAC to an excited state that was formed after ESIDPT. In this reaction, protons are transferred from the donor amide groups to the nitrogen acceptor atoms in both pyridyl rings. A similar conclusion was previously reached for the polar analogue compound of DAC, **2b**, which contains polar $-(O(C_2H_4O)_7Me)$ groups at the positions of the apolar $-(OC_{12}H_{25})$ groups.[1] As for **2b**, information concerning the kinetics of the ESIDPT process in DAC could be extracted from the time dependence of its fluorescence.

The emission spectrum of DAC in *n*-heptane (Figure 3) displays a rapid decay in the blue (λ < 450 nm) and a simultaneous rise near 530 nm. Considering that the DAC molecule undergoes an ESIDPT process, it is likely that the

rise near 530 nm is characteristic of the formation of the product state in the DPT process. Since the characteristic time of this process is ~200 fs (Table 1), we consider this as typical of the double proton-transfer process. Evidently, the band emission near 420 nm (with a ~200 fs decay time) is due to the precursor (reactant) state of the DPT product state. In the femtosecond fluorescence upconversion experiments, excitation is near 27 000 cm^{-1} and the short-living emission has its estimated maximum near 25 000 cm^{-1}, so DPT is in part accompanied by some very fast vibrational relaxation. The very fast DPT and vibrational relaxation are indicative of a highly asymmetric electronic potential energy surface that gives rise to a very fast redistribution of the initially excited (Franck−Condon) vibrational wave packet.

For DAC in chloroform, the blue-band emission initially shows a dynamic red-shift concomitant with its ~200 fs decay (Figure 3). Inhomogeneities in the solvation layer around the solute could sensitively affect the asymmetry of the excited-state electronic potential energy surface and thus the vibrational wave packet prepared by the exciting laser pulses. This, in turn, could give rise to an inhomogeneity in the decay time of the reactant state due to DPT. We interpret the dynamic red shift (with a typical time of ~500 fs) for DAC in chloroform (Figure 3) as due to an inhomogeneity in the decay time, the faster times being characteristic of molecules emitting more to the blue. Alternatively, one could consider a dynamic Stokes shift that is caused by solvation dynamics but this is considered to be a minor effect because of the small dipole moment of the solute in the excited state.

The time dependence of the polarized fluorescence transients of DAC (Figure 4) is further support for the aforementioned picture. The initial ~200 fs decay components in the parallel- and perpendicular-polarized transients are observed only for detection at 470 nm, i.e., the shortest detection wavelength possible in the upconversion experiment when excitation is at 380 nm. This wavelength of 470 nm is in the region where the trailing edges of the 420 nm and the 550 nm bands show overlap. Since the 420 nm emission band is attributed to the reactant state, it is not surprising that its rapid decay resulting from DPT is also manifested in the polarized emission.

The initial anisotropy at 470 nm is found as $r(0) \sim 0.25$, i.e., lower than the limiting value of 0.4. The latter may be expected when the emission is completely due to the initially excited Franck−Condon state because for this case the absorptive and emissive dipoles are parallel. The lower value for $r(0)$ must be due to the fact that at 470 nm the product state also contributes to the anisotropy. Evidently, the initial anisotropy in the fluorescence from the product state is much smaller than 0.4. In summary, we conclude that (i) the excited states of the reactant and product states have different electronic character (as expected) and (ii) the change in anisotropy has been reached within ~200 fs, thus illustrating that relaxation of the FC excited state on account of DPT is an ultrafast process.

The fluorescence anisotropy decay of DAC is biexponential (Table 2). The first component, with $\tau_1 \approx 20$ ps, is similar to the 2−25 ps decay components also found in the fluorescence transients measured under magic angle conditions (Table 1). It is likely that the decay in the time range of 2−25 ps is caused by the cooling of vibrationally hot DAC "product" molecules, i.e., these molecules, produced after ESIDPT, lose their excess vibrational energy by energy dissipation to the bath of solvent molecules. Usually this cooling takes place on a ps time scale.[43−47] The similar decay component in the fluorescence anisotropy reveals that vibrational cooling is accompanied by electronic relaxation. Thus vibronic rather than "pure" vibrational cooling occurs and this is as expected for an asymmetrically shaped excited-state potential energy surface.

Finally, we discuss the long decay components in the emission of DAC in *n*-heptane and chloroform. The decay times (in the experiments under magic angle conditions) of 200 ps for DAC in *n*-heptane and 120 ps for DAC in chloroform (Table 1) are typical of the lifetimes of the molecules in the relaxed excited product state. These times are comparable to those of the polar analogue of DAC, **2b**, with $-(O(C_2H_4O)_7Me)$ groups at the positions of the apolar $-(OC_{12}H_{25})$ groups in the nonaggregated (molecularly dissolved) form.[1] At first sight somewhat surprisingly, longer decay components are found for the fluorescence depolarization, ~300 ps for DAC in *n*-heptane and ~400 ps in chloroform. However, these times are characteristic of the rotational diffusion motions of the solute in the respective solvents. Such motions may be slower than the excited-state decay so that the fluorescence anisotropy does not completely disappear during the excited-state lifetime.

From a comparison of Figures 1 and 4 it can be seen that the absorption and emission spectra of TAB and DAC are similar. As noted above, the lowest transitions in the spectrum of DAC involve $\pi - \pi^*$ transitions of the bipyridine group. Also TAB contains bipyridine groups and by analogy we attribute the lowest spectral transitions of TAB (Figure 4) to arise from $\pi - \pi^*$ transitions in these functional groups.

The first absorption band of TAB is sensitive to the polarity of the solvent. Whereas in chloroform this band is unstructured and the band maximum is near 350 nm, in *n*-heptane the band is structured and its maximum is near 365 nm. In apolar solvents, the absorption spectrum of TAB exhibits a Cotton effect.[2] From this it was concluded that TAB molecules in apolar solvents are aggregated in a chiral fashion. We attribute the red shift of the first absorption band and the presence of fine structure when TAB is dissolved in an apolar solvent to the self-assembling of the TAB molecules.

As discussed above, for DAC the Stokes shift of ~10 000 cm^{-1} of its band emission relative to the first absorption band is caused by an ESIDPT. For TAB, in the aggregated state as well as in the nonaggregated state, a similar shift of ~10 000 cm^{-1} of the steady-state emission band is observed (Figure 4). We infer that for TAB the ESIDPT process exists not only in the nonaggregated (molecular) state, but also in the aggregated state. Recently, chirality of self-assembled stacks of C_3-symmetrical disk-shaped molecules **1b** with a structure analogous to that of TAB was demonstrated.[1] The stacks result from the combined action of cooperative hydrogen bonding and $\pi-\pi$ intermolecular interactions. Similarly, also in the case of TAB, aggregation might result from such interactions. Thus, the role of the amide hydrogen atoms in the bipyridyl cores is 2-fold: hydrogen atoms are involved in aggregation and in ESIDPT.

Contrary to the S_0-S_1 absorption (350−380 nm), the steady-state fluorescence band maximum near 530 nm is not shifted upon aggregation. This implies that the energy difference of the emissive and ground states of the tautomer is not influenced by aggregation. The absence of a spectral shift, when comparing the emissions from the aggregated and nonaggregated species, suggests that the emission from the aggregate originates in a localized emissive state. On the other hand, upon aggregation, the first absorption band of TAB undergoes a red shift and exhibits fine structure. The red shift is suggestive of a delocalized nature of the excited Franck−Condon state;[5,9,25,48,49] the fine structure hints to a relatively strict structure of the aggregate for which the absorption is not blurred by inhomogeneous

broadening. It is likely that the ESIDPT process is accompanied by localization (trapping)[13,50−52] of the excitation (possibly at one of the diamino-bipyridyl groups) within the TAB aggregate. Excitation localization after DPT is not surprising since the geometry of the molecule within the aggregate at which the excitation is trapped differs from that of the neighboring molecules in the aggregate and consequently its excited state is nonresonant with the excited states of the nearest neighboring molecules in the aggregate, so that exciton delocalization cannot occur.

The results of the femtosecond fluorescence upconversion experiments of nonaggregated TAB, in chloroform, are comparable to those of DAC. Just as for DAC, a ∼200−300 fs decay of the 430 nm emission and a simultaneous rise of the 530 nm band, associated with the product after DPT, is observed in the transients (Table 3). The observed kinetics is characteristic of the ESIDPT process. As in the case of DAC, the fast decay components in the transients of TAB in chloroform detected in the blue part of the emission (420−470 nm) become slightly slower at longer detection wavelengths. This produces a dynamic red shift in the blue wing of the reconstructed emission spectrum (Figure 6, lower panel), with a characteristic time of less than ∼1 ps. The dynamic red shift may be due to some inhomogeneity in the emission spectrum, and associated with this, an inhomogeneity in the lifetime of the reactants in the ESIDPT process so that, as time progresses, the more reddish emission of the longer lived species becomes more prominent. As discussed above for DAC, the longer time constants in the fluorescence decay kinetics, in the 3−25 ps range, are attributed to vibrational cooling. This is not accompanied by a dynamic Stokes shift and takes place after the ESIDPT process.

We now consider the excited-state dynamics of TAB, dissolved in *n*-heptane, i.e., the solution now contains TAB in the aggregated form. The ∼300 fs decay of the emission near 430 nm and the concomitant rise near ∼530 nm (Table 3) are characteristic of the ESIDPT process in aggregated TAB. The similar excited-state proton-transfer times of aggregated and nonaggregated TAB show that aggregation is of little influence on the proton translocation time, although in the aggregate the process seems somewhat slower. The small dynamic red shift of the blue-wing emission observed for nonaggregated TAB remained unresolved for the TAB/*n*-heptane solution. This could indicate that the inhomogeneity of the TAB stack structure is less than that for TAB molecularly dissolved in chloroform.

The additional ∼3−25 ps components found in the fluorescence transients of TAB in *n*-hexane are, as for nonaggregated TAB and DAC, typical of thermalization of the vibrational energy with the surrounding bath and are thus attributed to vibrational cooling.[3,4,43−47] The narrowing of the band emission (Figure 6, upper panel) on the same time scale illustrates that vibrational relaxation is accompanied by a narrowing of the spectral density distribution.

The polarized fluorescence transients observed for TAB at 470 nm (Figure 9) show a decay behavior in which a fast component with ∼200 fs decay is lacking. This is particularly clear from the transients recorded with a time window of 8 ps: the fastest decay component has a time constant of ∼1 ps. While for DAC the trailing edges of the 420 and 550 nm bands show overlap, this is not the case for TAB (Figure 5), not even at the earliest times of ∼200 fs of our measurements (Figure 7). Thus, for DAC, at 470 nm very fast polarized transients representative of DPT cannot be observed.

For aggregated TAB in *n*-heptane the initial anisotropy was found as $r(0) \approx 0.25$. According to the expression $r(t) = 0.6 \cos^2\beta(t) - 0.2$, relating the anisotropy, $r(t)$, to the angle β between the directions for the transition dipole moments of absorption and emission, we estimate that the dipole moment for the Franck−Condon excitation lies at about 35° from the direction of the emissive transition dipole prior to ESIDPT. The initial anisotropy of ∼0.25 measured for aggregated TAB is comparable to that of DAC and nonaggregated TAB (in chloroform). This is in support of the above-mentioned idea that the photoexcitation almost immediately (within ∼100 fs) becomes trapped at a TAB diamino-bipyridyl group.

The fluorescence anisotropy decay of aggregated TAB is biexponential, with typical times of 1.0 and 20 ps. The contribution of the 1 ps depolarization component is appreciable (35%). The component is not observed under magic angle conditions, however. Furthermore, it was verified that for nonaggregated TAB (in chloroform) the 1 ps component is also lacking. The fast depolarization must therefore be characteristic of only the TAB aggregates. Since the decay of the integrated aggregate emission in the first few picoseconds is negligible (the lifetime is ∼4 ns), it is proposed that some excited-state energy transfer causes the fast fluorescence depolarization component in the aggregates. Energy migration within dendrimers and aggregates is known to give rise to fluorescence depolarization on time scales from subpicosecond[4,6,9−11,21] to tens of picoseconds.[3,26,27,53,54] It is likely that the 1 ps fluorescence depolarization is due to excited-state energy transfer between nearest-neighbor chromophores within the aggregate. For arranged symmetrical aggregate structures such as disks, rings, and helices, the final anisotropy for excitations after random diffusion (not considering orientation diffusion) is ∼0.1.[10,22] The observed anisotropy of ∼0.1 after about 1 ps for aggregated TAB is in agreement with a fast randomization of the initial polarization through energy transfer among adjacent chromophores in the aggregate until the excitation is trapped at a pyridine site within the TAB stack. As illustrated in Figure 9, a further lowering of the anisotropy to ∼0.07 is observed with a time of ∼20 ps at longer times (40 ps window). The ∼20 ps fluorescence anisotropy decay component of TAB aggregates is, as in the case of DAC, attributed to vibrational cooling. Naturally, thermalization of vibrationally "hot" states by energy exchange with the bath can affect the fluorescence polarization only provided the cooling involves electronic relaxation as well. Thus, vibronic rather than "pure" vibrational relaxation takes place in due time after trapping of the excitation within the TAB aggregates.

Finally, we briefly discuss the long fluorescence decay components obtained in magic angle upconversion and TCSPC experiments (τ_4 and τ_5, Table 3). The lifetime component, τ_5, is appreciably lengthened from ∼0.3 ns to ∼4 ns upon aggregation of the TAB molecules. A similar lifetime lengthening has previously been observed for chirally stacked discotics **1b**.[1] The lengthening of the lifetime probably results from a more rigid structure of the aggregated molecular system so that low-frequency motions, which modulate the propeller-type structure of nonaggregated TAB, are suppressed. The lifetime of the fluorescent state of TAB in nonaggregated as well as aggregated forms may not be well defined. As pointed out above, the results for the optical band spectra as well as the fast kinetics of the fluorescence for nonaggregated TAB molecules indicated the existence of structural inhomogeneities. These could also affect the lifetime of the excited state and a spread of lifetimes in the range from ∼100 to ∼400 ps for nonaggregated **1a** and **2a** and ∼0.1 to ∼4 ns for aggregated **1a** may arise. The slow tail of the fluorescence transients of TAB

in chloroform is thus considered as a multiexponential decay rather than as a biexponential, τ_4 and τ_5 being merely indicative of the spread in the excited-state lifetimes.

Conclusion

We have studied the fluorescence kinetics of the C_3-symmetrical disk TAB (**1a**) and its subgroup molecule DAC (**2a**), dissolved in polar and apolar liquids, applying the femtosecond fluorescence upconversion technique. The results show that **1a** and **2a** exhibit excited-state intramolecular double proton transfer (ESIDPT) with a typical time of ∼200−300 fs; in **1a**, ESIDPT takes place for the molecule in the aggregated as well as the nonaggregated state. Apparent dynamic Stokes shifts were measured with a typical time of a few hundred femtoseconds. The shifts are attributed to structural inhomogeneities of molecularly dissolved conformers of **1a** and **2a**.

The fluorescence decay of the photoproduct states of **1a** and **2a** is multiexponential, with an initial decay in the range of 3 to 25 ps. These times are characteristic of the cooling of vibrationally hot "product" states in which excess vibrational energy is lost by energy dissipation to the bath of solvent molecules. From fluorescence depolarization measurements it could be demonstrated that depolarization occurs in part with a typical time of ∼20 ps. It is concluded that vibrational cooling in the excited state is accompanied by electronic relaxation, making the cooling process essentially a vibronic relaxation process. Fluorescence anisotropy measurements of **1a** in the aggregated state revealed a fast ∼1 ps decay component, not observed for molecularly dissolved **1a** and **2a**. The rapid depolarization component is discussed to be representative of an excited-state energy transfer among neighboring disk molecules in the stacks.

Finally, multiexponential lifetime decays are observed for molecularly dissolved **1a** and **2a** (0.1−0.4 ns) and aggregated **1a** (0.1−4 ns). The spread in lifetimes is attributed to structural inhomogeneities of the molecules and stacks in solution. The significant lengthening of the average excited-state lifetime in TAB upon aggregation by an order of magnitude results from a more rigid structure of the aggregated molecular system so that low-frequency motions, which modulate the propeller-type structure of nonaggregated TAB, are suppressed.

Acknowledgment. The authors thank Professor E. W. Meijer and Dr. J. A. J. M. Vekemans (Eindhoven University of Technology) for valuable discussions and support.

References and Notes

(1) Brunsveld, L.; Zhang, H.; Glasbeek, M.; Vekemans, J. A. J. M.; Meijer E. W. *J. Am. Chem. Soc*. **2000**, *122*, 6175 and references therein.

(2) Palmans, A. R. A.; Vekemans, J. A. J. M.; Havinga, E. E.; Meijer, E. W. *Angew. Chem., Int. Ed. Engl.* **1997**, *36*, 2648.

(3) Lim, S. H.; Bjorklund, T. G.; Bardeen, C. J. *Chem. Phys. Lett.* **2001**, *342*, 555.

(4) Kano, H.; Kobayashi, J. *J. Chem. Phys*. **2002**, *116*, 184.

(5) Lampoura, S. S.; Spitz, C.; Dähne, S.; Knoester, J.; Duppen, K. *J. Phys. Chem. B* **2002**, *106*, 3103.

(6) Prokhorenko, V. I.; Steensgaard, D. B.; Holzwarth, A. R. *Biophys. J.* **2000**, *79*, 2105.

(7) Leegwater, J. A. *J. Phys. Chem.* **1996**, *100*, 14403.

(8) Dahlbom, M.; Pullerits, T.; Mukamel, S.; Sundström, V. *J. Phys. Chem. B* **2001**, *105*, 5515.

(9) Book, L. D.; Ostafin, A. E.; Ponomarenko, N.; Norris, J. R.; Scherer, N. F. *J. Phys. Chem. B* **2000**, *104*, 8295.

(10) Varnavski, O. P.; Ostrowski, J. C.; Sukhomlinova, L.; Twieg, R. J.; Bazan, G. C.; Goodson, T., III *J. Am. Chem. Soc*. **2002**, *124*, 1736.

(11) Varnavski, O. P.; Samuel, I. D. W.; Pålsson, L.-O.; Beavington, R.; Burn, P. L.; Goodson, T., III *J. Chem. Phys.* **2002**, *116*, 8893.

(12) Polívka, T.; Pullerits, T.; Herek, J. L.; Sundström, V. *J. Phys. Chem. B* **2000**, *104*, 1088.

(13) Kim, J.; Unterreiner, A.-N.; Rane, S.; Park, S.; Jureller, J.; Book, L.; Liau, Y. H.; Scherer, N. F. *J. Phys. Chem. B* **2002**, *106*, 12866.

(14) Ohta, K.; Yang, M.; Fleming, G. R. *J. Chem. Phys.* **2001**, *115*, 7609.

(15) Kühn, O.; Sundström, V. *J. Chem. Phys.* **1997**, *107*, 4154.

(16) Meier, T.; Zhao, Y.; Chernyak, V.; Mukamel, S. *J. Chem. Phys.* **1997**, *107*, 3876.

(17) Spitz, C.; Knoester, J.; Ouart, A.; Daehne, S. *Chem. Phys.* **2002**, *275*, 271.

(18) Hughes, R. E.; Hart, S. P.; Smith, D. A.; Movaghar, B.; Bushby, R. J.; Boden, N. *J. Phys. Chem. B* **2002**, *106*, 6638.

(19) Ruseckas, A.; Theander, M.; Andersson, M. R.; Svensson, M.; Prato, M.; Inganäs, O.; Sundström, V. *Chem. Phys. Lett.* **2000**, *322*, 136.

(20) Ern, J.; Bock, A.; Marcel, L. O.; Rengel, H.; Wegner, G.; Trommsdorff, H. P.; Kryschi, C. *J. Phys. Chem. A* **1999**, *103*, 2446.

(21) Ranasinghe, M. I.; Murphy, P.; Lu, Z.; Huang, S. D.; Twieg, R. J.; Goodson, T., III *Chem. Phys. Lett.* **2003**, *383*, 411.

(22) Jiminez, R.; Dikshit, S. N.; Bradforth, S. E.; Fleming, G. R. *J. Phys. Chem.* **1996**, *100*, 6825.

(23) Cho, H. S.; Song, N. W.; Kim, Y. H.; Jeoung, S. C.; Hahn, S.; Kim, D.; Kim, S. K.; Yoshida, N.; Osuka, A. *J. Phys. Chem. A* **2000**, *104*, 3287.

(24) Kumble, R.; Palese, S.; Visschers, R. W.; Dutton, P. L.; Hochstrasser, R. M. *Chem. Phys. Lett.* **1996**, *261*, 396.

(25) Lee, J. H.; Min, C. K.; Joo, T. *J. Chem. Phys*. **2001**, *114*, 377.

(26) Rubtsov, I. V.; Kobuke, Y.; Miyaji, H.; Yoshihara, K. *Chem. Phys. Lett.* **1999**, *308*, 323.

(27) Glasbeek, M.; Zhang, H. *Chem. Rev*. **2004**, *104*, 1929.

(28) Mialocq, J.-C.; Gustavsson, T. In *New Trends in Fluorescence Spectroscopy*; Valeur, B., Brochon, J.-C., Eds.; Springer: Heidelberg, Germany, 2001; pp 61−80.

(29) Nagarajan, V.; Johnson, E. T.; Williams, J. C.; Parson, W. W. *J. Phys. Chem. B* **1999**, *103*, 2297.

(30) Toele, P.; Zhang, H.; Glasbeek, M. *J. Phys. Chem. A* **2002**, *106*, 3651.

(31) Palmans, A. R. A.; Vekemans, J. A. J. M.; Fisher, H.; Hikmet, R. A.; Meijer, E. W. *Chem. Eur. J.* **1997**, *3*, 300. Palmans, A. R. A.; Vekemans, J. A. J. M.; Fisher, H.; Hikmet, R. A.; Meijer, E. W. *Adv. Mater*. **1998**, *10*, 873.

(32) Middelhoek, E. R.; van der Meulen, P.; Verhoeven, J. W.; Glasbeek, M. *Chem. Phys.* **1995**, *198*, 373. Zhang, H.; Jonkman, A. M.; van der Meulen, P.; Glasbeek, M. *Chem. Phys. Lett.* **1994**, *224*, 551.

(33) Maroncelli, M.; Fleming, G. R. *J. Chem. Phys.* **1987**, *86*, 6221.

(34) Lakowicz, J. R. *Principles of Fluorescence Spectroscopy*, 2nd ed.; Kluwer Academic/Plenum Publishing: New York, 1999.

(35) Bulska, H. *Chem. Phys. Lett.* **1983**, *98*, 398.

(36) Neuwahl, F. V. R.; Foggi, P.; Brown, R. *Chem. Phys. Lett.* **2000**, *319*, 157.

(37) Marks, D.; Prosposito, P.; Zhang, H.; Glasbeek, M. *Chem. Phys. Lett.* **1998**, *289*, 535.

(38) Marks, D.; Zhang, H.; Glasbeek, M.; Borowicz, P.; Grabowska, A. *Chem. Phys. Lett.* **1997**, *275*, 370.

(39) (39) Wortmann, R.; Elich, K.; Lebus, S.; Liptay, W.; Borowicz, P.; Grabowska, A. *J. Phys. Chem.* **1992**, *96*, 9724.

(40) (40) Borowicz, P.; Grabowska, A.; Wortmann, R.; Liptay, W. *J. Lumin.* **1992**, *52*, 265.

(41) Barone, V.; Adamo, C. *Chem. Phys. Lett.* **1995**, *241*, 1.

(42) Sobolewski, A. L.; Adamowicz, L. *Chem. Phys. Lett.* **1996**, *252*, 33.

(43) Elsaesser, T.; Kaiser, W. *Annu. Rev. Phys. Chem.* **1991**, *42*, 83.

(44) Arzhantsev, S. Y.; Takeuchi, S.; Tahara, T. *Chem. Phys. Lett.* **2000**, *330*, 83.

(45) Toele, P.; Zhang, H.; Glasbeek, M. *Chem. Phys. Lett.* **2003**, *368*, 66.

(46) Fujino, T.; Arzhantsev, S. Y.; Tahara, T. *J. Phys. Chem. A* **2001**, *105*, 8123.

(47) Chou, P. T.; Chen, Y. C.; Yu, W. S.; Chou, Y. H.; Wei, C. Y.; Cheng, Y. M. *J. Phys. Chem. A* **2001**, *105*, 1731.

(48) Evans, C. E.; Bohn, P. W. *J. Am. Chem. Soc.* **1993**, *115*, 3306.

(49) Knapp, E. W. *Chem. Phys.* **1984**, *85*, 73.

(50) Cho, H. S.; Yang, S. I.; Kim, S.-K.; Shin, E. J.; Kim, D. *J. Phys. Chem. B* **1999**, *103*, 6504.

(51) Freiberg, A.; Rätsep, M.; Timpmann, K.; Trinkunas, G. *J. Lumin.* **2003**, *102*, 363.

(52) Grage, M. M.-L.; Zaushitsyn, Y.; Yartsev, A.; Chachisvillis, M.; Sundström, V.; Pullerits, T. *Phys. Rev. B* **2003**, *67*, 205207.

(53) Latterini, L.; de Belder, G.; Schweitzer, G.; van der Auweraer, M.; de Schryver, F. C. *Chem. Phys. Lett.* **1998**, *295*, 11.

(54) Zhang, J. Z.; Kreger, M. A.; Hu, Q.-S.; Vitharana, D.; Pu, L.; Brock, P. J.; Scott, J. C. *J. Chem. Phys.* **1997**, *106*, 3710.